Available online at www.sciencedirect.com
SCIENCE DIRECT®
PERGAMON
International Journal of Multiphase Flow 29 (2003) 559–578
International Journal of Multiphase Flow
www.elsevier.com/locate/ijmulflow

Influence of electric field on single gas-bubble growth and detachment in microgravity

P. Di Marco [a,*], W. Grassi [a,1], G. Memoli [a,1], T. Takamasa [b,2], A. Tomiyama [c,3], S. Hosokawa [c,3]

[a] *LOTHAR, Department of Energetics, "L. Poggi", University of Pisa, Italy via Diotisalvi 2, I-56126 Pisa, Italy*
[b] *Department of Marine Engineering, Faculty of Marine Science, Tokyo University of Mercantile Marine, Japan*
[c] *Graduate School of Science and Technology, Kobe University, Japan 1-1, Rokkodai, Nada, Kobe 657-8501, Japan*

Received 8 August 2002; received in revised form 3 February 2003

Abstract

The effect of electric and gravitational field on detachment and motion of gas bubbles was studied by injecting nitrogen in a fluoroinert liquid (FC-72) at ambient temperature and pressure through an orifice (about 0.1 mm diameter) drilled in a horizontal tube. In such a way, it was possible to investigate the mechanical effects in bubble dynamics separately from the thermal and mass exchange ones involved in boiling. An electric field of nearly cylindrical geometry was generated around the tube by imposing a D.C. potential drop V (0–18 kV) to a eight-rod cylindrical "squirrel cage" surrounding it. The apparatus was operated in microgravity conditions in the dropshaft of JAMIC in Hokkaido, Japan. Bubble size, detachment frequency and velocity were measured by digital processing of high-speed video images. The results showed that in the absence of electric field bubble detachment did not take place at low gas flow rate; conversely at higher gas flow, the dynamical effects were sufficient to induce bubble detachment even in the absence of the buoyant force. The application of electric field was confirmed to be effective in promoting bubble detachment at values of diameter greater but of the same order of magnitude as in normal gravity, and in providing a force to remove the bubbles away from the orifice.

Keywords: Bubble formation; Bubble departure volume; Electrohydrodynamics; Electric field; Microgravity

* Corresponding author. Tel.: +39-050-569610; fax: +39-050-569666.
E-mail addresses: lothar@ing.unipi.it (P. Di Marco, W. Grassi, G. Memoli), takamasa@ipc.tosho-u.ac.jp (T. Takamasa), tomiyama@mech.kobe-u.ac.jp (A. Tomiyama), hosokawa@mech.kobe-u.ac.jp (S. Hosokawa).
[1] Tel.: +39-050-569646; fax: +39-050-830116.
[2] Tel.: +81-3-5245-7406; fax: +81-3-5245-7336.
[3] Tel.: +81-78-803-6132; fax: +81-78-803-6155.

0301-9322/03/$ - see front matter
doi:10.1016/S0301-9322(03)00030-2

1. Introduction

The production of bubbles from a submerged orifice plays a fundamental role in the comprehension of phenomena which involve mass and thermal exchange, both industrial (absorbers, fermenters, chemical reactors, carbonated beverages, mineral processing) and natural (underwater currents and volcanoes, as an example). Experimental and theoretical work on this topic is useful for the optimization of terrestrial industrial processes and for two-phase flow applications in aerospace technology. Bubble behavior in space is also important for life-support systems and containerless technology. The presence of an electric field, which may replace the lacking buoyancy, can be helpful in this field as a gas/vapor management tool.

In particular, it is well established that the application of an external electric field enhances pool boiling performance and augments the critical heat flux, see e.g. Di Marco and Grassi (1993), Allen and Karayiannis (1995). These effects were largely tested for the applications in normal gravity conditions since early 1960s and are now mature for industrial development. Furthermore, this technique may have important application in microgravity heat transfer devices, since a very low amount of energy is required to establish the electrostatic field. An electric field of appropriate geometry may reduce the size of bubbles and drive them away from the surface. The tests conducted in parabolic flight by Di Marco and Grassi (1999) demonstrated that pool boiling was stabilized by the action of the field and, for a higher enough applied voltage, the same beneficial effect on critical heat flux enhancement as in normal gravity applications was confirmed. The main achievements on the study of pool boiling in microgravity were summarized by Di Marco and Grassi (2001, 2002). The modeling of boiling in the presence of an electric field is not straightforward due to the great complexity of the involved physical phenomena and requires a clear identification of the forces acting on a detaching bubble. Therefore, experiments performed in a simple configuration help in clarifying the effect of the electrical force on bubbles, by getting rid of the effects of thermal gradients and mass transfer between the two phases.

Considering the above-mentioned motivations, a simple experimental facility has been set up to investigate the evolution of nitrogen bubbles in an isothermal pool of FC-72 in the presence of an externally applied electric field, under the action of terrestrial gravity or less.

1.1. State of the art

The phenomena of detachment and rise of gas bubbles in a stagnant liquid were extensively studied experimentally starting from 1960s, see e.g. the pioneeristic studies of Datta et al. (1950), Peebles and Garber (1953), Davidson and Schuler (1960a,b), Ramakrishnan et al. (1969), Khurana and Kumar (1969), Satyanarayan et al. (1969), Wraith (1971) and Terasaka and Tsuge (1993). The earlier works were summarized by Clift et al. (1978) and recently by Magnaudet and Eames (2000). All of these studies were performed using two-component immiscible fluids (gas into liquid), in adiabatic conditions, and most of them were related to the motion of air bubbles in water or water-based mixtures. Only a few works focused on different fluids (e.g. Park et al., 1977; Tsuge and Hibino, 1972). To the authors' knowledge, bubbling phenomena in a stagnant fluid (water) in microgravity were experimentally investigated only by Pamperin and Rath (1995), by Tsuge et al. (1997) and recently by Herman et al. (2002), who used an organic fluid and included the effect of an electric field on the phenomenon.

1.2. Models for bubble dynamics

A large amount of theoretical models for bubble formation, detachment and rise velocity are available, see e.g. Peebles and Garber (1953) Davidson and Schuler (1960a,b), Ramakrishnan et al. (1969), Satyanarayan et al. (1969), Kumar and Kuloor (1970), Wraith (1971), Tsuge (1986), Tomiyama (1998) and Tomiyama et al. (1998). The evolution of a gas bubble immersed in a liquid of different nature and attached to an orifice (see Fig. 1) can be studied by considering the gas volume V_B, bounded by the surface A_B (gas-liquid interface) and A_o (orifice inlet), joined by the three-phase contact line L. If the evaporation of the liquid into the gas and the dissolution of gas in the liquid are negligible, the surface A_B can be considered adiabatic to mass. The mass and momentum balances for this system are

$$\frac{\mathrm{d}}{\mathrm{d}t}\int_{V_B}\rho_G\,\mathrm{d}V = -\int_{A_o}\rho_G(\mathbf{u}_G\cdot\mathbf{n})\,\mathrm{d}A \tag{1}$$

$$\frac{\mathrm{d}}{\mathrm{d}t}\int_{V_B}\rho_G\mathbf{u}_G\,\mathrm{d}V = -\int_{A_o}\rho_G\mathbf{u}_G(\mathbf{u}_G\cdot\mathbf{n})\,\mathrm{d}A + \int_{V_B}\rho_G\mathbf{g}\,\mathrm{d}V - \int_{A_B}(\boldsymbol{\Sigma}_B\cdot\mathbf{n})\,\mathrm{d}A - \int_{A_o}(\boldsymbol{\Sigma}_o\cdot\mathbf{n})\,\mathrm{d}A + \int_L(\boldsymbol{\sigma}_{12}+\boldsymbol{\sigma}_{23}+\boldsymbol{\sigma}_{31})\,\mathrm{d}L \tag{2}$$

where ρ_G is the gas density, $\mathbf{u}_G$ the gas velocity, V_B the bubble volume, A_o the orifice area, L the orifice perimeter, $\boldsymbol{\Sigma}$ the stress tensor acting on the bounding surfaces (gas–liquid, B and orifice, o) $\boldsymbol{\sigma}_{ij}$ the surface tension (vector, oriented tangentially to the surface separating the phases i and j and perpendicular to the contact line), $\mathbf{n}$ the unit outward normal to the bubble surface and $\mathbf{g}$ the acceleration of gravity. When the bubble detaches, the surface area of the orifice, A_o, is set to zero and the last two terms of Eq. (2) vanish. The momentum jump condition across the interface, neglecting the gradients of surface tension, is (Delhaye, 1980)

$$\boldsymbol{\Sigma}_G\cdot\mathbf{n} = \boldsymbol{\Sigma}_L\cdot\mathbf{n} + \sigma\kappa\mathbf{n} \tag{3}$$

where σ is the surface tension and κ is the sum of the two principal surface curvatures

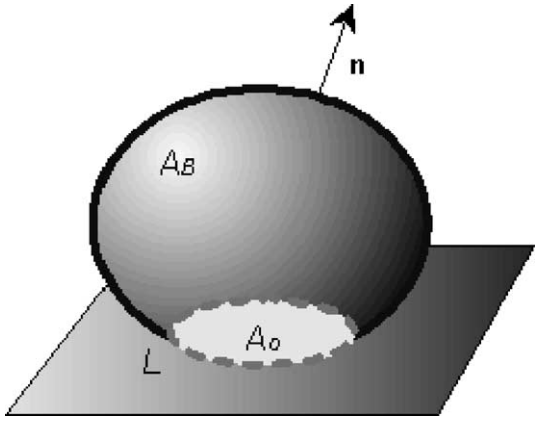

Fig. 1. Sketch of the considered system.

$$\kappa = \frac{1}{R_1} + \frac{1}{R_2} \tag{4}$$

It has to be accounted that the pressure of the liquid p_L is due to the contribution of the hydrostatic pressure, of the form drag and of the inertial action of the liquid surrounding the bubble, which counteracts its expansion.

Such an approach meets with several difficulties in calculating the integrals in RHS of Eq. (2) along a moving boundary and, at present, is useful only for numerical modeling purposes. The momentum balance along the vertical (x) direction is thus rewritten as

$$\frac{\mathrm{d}}{\mathrm{d}t}[V_B(\rho_G + C_M\rho_L)u_B] = (\rho_L - \rho_G)V_B g - F_D - \pi d_o \sigma \sin\theta + \int_{A_o} \rho_G u_{in}^2 \,\mathrm{d}A + \frac{\pi d_o^2}{4}(p_G - p_L) + F_E \tag{5}$$

where u_B is the velocity of the center of mass of the bubble, u_{in} the inlet gas velocity at the orifice, θ the contact angle and d_o the diameter of the injection orifice. The hypotheses underlying this approach are thoroughly reviewed by Buyevich and Webbon (1996). The terms in RHS represent the buoyancy, the drag, the contact force along the three-phase line (where θ is the actual contact angle at the surface, not necessarily the equilibrium one), the momentum inflow through the orifice, the unbalanced excess of internal pressure and the expansion force, respectively. All the models proposed for bubble growth and detachment are based on Eq. (5), though some terms have been often neglected. To make use of Eq. (5), a geometry for the growing bubble has to be assumed: the bubble is generally schematized as a segment of sphere, or a sphere attached to a cylindrical stem. Semi-empirical constitutive models are necessary to represent at least the terms C_M (virtual mass coefficient), F_D (drag force), F_E (expansion force). Generally C_M is given as 0.5 for a nozzle orifice and 11/16 for a sphere attached to a plane (Milne Thomson, 1996); a correction factor to these values has been introduced by Buyevich and Webbon (1996). The contribution due to the inertia of the gas, represented by ρ_G on LHS of Eq. (5), is always neglected.

The expansion force over a gas sphere in a quiescent liquid is modeled after Rayleigh (1920) as (Buyevich and Webbon, 1996)

$$F_E = -\frac{\pi d_o^2}{4}\rho_L\left[R_B\frac{\mathrm{d}^2R_B}{\mathrm{d}t^2} + \frac{3}{2}\left(\frac{\mathrm{d}R_B}{\mathrm{d}t}\right)^2\right] \tag{6}$$

It is worth noting that only the contribution pertinent to the orifice is not self-balanced and has to be considered here.

Several models have been developed for the drag force, accounting for the system geometry and the flow regime. The drag force has been neglected during the growth and detachment phase by several authors (Wraith, 1971; Satyanarayan et al., 1969; Buyevich and Webbon, 1996). This force can be expressed as

$$F_D = \frac{1}{2}C_D\rho_L\frac{\pi d_{eq}^2}{4}u_B^2 \tag{7}$$

where C_D is the drag coefficient ad d_{eq} is the bubble equivalent diameter, i.e. the diameter of the sphere having the same volume as the bubble

$$d_{eq} = \sqrt[3]{\frac{6V_B}{\pi}} \tag{8}$$

As an example, Ramakrishnan et al. adopted for C_D the Stokes' equation for a viscous flow past a solid sphere

$$C_D = \frac{24}{Re} \tag{9}$$

Gaddis and Vogelpohl (1986) adopted

$$C_D = \frac{24}{Re} + 1 \tag{10}$$

and Pamperin and Rath (1995), considering the modified Stokes' equation for a viscous flow past a sphere corrected with the Hadamard–Rybczynski factor:

$$C_D = \frac{2}{3}\left(\frac{24}{Re} + \frac{4}{\sqrt{Re}}\right) + 0.4 \tag{11}$$

For this model, the velocity to be used in Eq. (7) and (11) is calculated at the bubble top ($u = 2u_B$).

It has to be remarked that Eq. (5) is able to account only in a simplified way for the actions exerted on the interface by the surrounding fluid. Eq. (5) keeps its validity after bubble detachment: in such a case, all the forces originating from the contact of the bubble with the orifice, namely the momentum inflow, the contact force, the excess pressure and the expansion force vanish.

Different bubble detachment criteria were adopted. Ramakrishnan et al. (1969) assumed that the detachment occurs when the bubble neck reaches a length equal to the bubble radius. A similar criterion (i.e., a limit distance between the bubble center and the orifice) was adopted by Davidson and Schuler (1960a,b), Khurana and Kumar (1969) and Wraith (1971). Buyevich and Webbon (1996) proposed that the hydrodynamic instability in the stem should be considered, without actually applying this consideration in their model, and ended up in adopting the Ramakrishnan's hypothesis. Other authors have assumed that detachment occurs when a force balance like Eq. (5) is no longer satisfied in the presence of the forces originating from the contact of the bubbles with the orifice. In particular, considering a force balance like Eq. (5), and neglecting all the terms but the third and the fourth in RHS (i.e., considering only surface tension and inlet momentum forces), the following criterion can be obtained

$$0 = -\pi d_o \sigma \sin\theta + \alpha \frac{\pi d_o^2}{4} \rho_G u_o^2 \tag{12}$$

where the parameter α depends upon the velocity profile in the inlet orifice. In particular, for a flat profile, $\alpha = 1$ while for a parabolic one $\alpha = 4/3$. Rearranging, a modified Weber number, We^*, is obtained

$$We^* = \frac{\rho_G u_0^2 d_o}{\sigma} = 4\frac{\sin\theta}{\alpha} \tag{13}$$

Pamperin and Rath (1995), by similar considerations, concluded that, assuming $\theta = \pi/2$, bubble detachment in the absence of gravity can occur only if

$$We^* > 8 \tag{14}$$

They claimed that the data from their experiment in droptower (referring to air bubbles in water, with injection orifices of 0.39 and 0.80 mm diameter) are in agreement with the derived criterion, Eq. (14). They observed detachment for $We^* > 10$ during the 4.74 s of microgravity available in their experiment.

To start the bubble formation, an excess pressure is necessary inside the gas injection chamber underlying the inlet orifice. The amount of such excess can be estimated by means of a static balance as

$$\Delta p = \frac{4\sigma}{d_o} \tag{15}$$

The inlet flow and pressure at the orifice, and thus the entire phenomenon, are influenced by the dynamics of the compressible gas volume constituted by the chamber. This is generally accounted for through the capacitance number N_c (Hughes et al., 1955)

$$N_c = \frac{4g\rho_L V_{ch}}{\pi d_o^2 (p_{ch} + \Delta p/2)} \tag{16}$$

where p_{ch} is the pressure in the chamber, of volume V_{ch}, and Δp is given by Eq. (15). It is generally agreed (Ramakrishnan et al., 1969) that low values of the capacitance number ($N_c < 1$) correspond to the so-called *constant flow conditions*, in which the inlet flow through the orifice is constant and there is no or very little waiting time between the detachment of a bubble and the beginning of formation of the next one; conversely, for $N_c > 10$ *constant pressure conditions* are established, in which the pressure in the chamber is nearly constant and the flow rate through the orifice undergoes significant oscillations.

For bubbles originating from the same orifice, it has been found experimentally that the detachment volume has a characteristic trend against the gas flow rate: initially the detachment volume is nearly constant even with increasing the flow rate (and thus the detaching frequency increases linearly with it) and almost independent of liquid viscosity. Afterwards, the detachment volume grows with inlet flow rate and according to Clift et al. (1978) it depends on liquid viscosity and increases with it. The data collected on ground with the present experimental apparatus are in agreement with this trend (Danti et al., 2000; Di Marco et al., 2001).

1.3. Effect of an electrostatic field on bubble dynamics

The most generally accepted expression for the volumic electric force that acts on a fluid, to be included in the momentum equation, is (Landau and Lifšitz, 1986)

$$\mathbf{F}_e = \rho_F \mathbf{E} - \frac{1}{2} E^2 \operatorname{grad} \varepsilon + \frac{1}{2} \operatorname{grad}\left[E^2 \rho \left(\frac{\partial \varepsilon}{\partial \rho} \right)_T \right] \tag{17}$$

where E is the electric field intensity, ε the electrical permittivity of the medium and ρ_F the free charge density.

Only the first term (Coulomb's force) depends on the sign of the electric field. It is present when free charge buildup occurs and in such cases it generally predominates over the other electrical forces. The other two terms depend on the gradient of the electric field and of the dielectric

constant (related to thermal gradients or phase discontinuities), and on the magnitude of E^2 thus being independent of the field polarity. The second term is a body force due to non-homogeneities of the dielectric constant and the third term is caused by non-uniformities in the electric field distribution.

In the absence of free charge, the net force acting on a ellipsoidal gas bubble can be simply expressed as (Landau and Lifšitz, 1986),

$$F_{\mathrm{DEP}} = \frac{\pi}{6} d_{\mathrm{eq}}^3 \frac{\varepsilon_{\mathrm{G}} - \varepsilon_{\mathrm{L}}}{n_1 \varepsilon_{\mathrm{G}} + (1 - n_1)\varepsilon_{\mathrm{L}}} \varepsilon_{\mathrm{L}} \ \mathrm{grad}\, E^2 \tag{18}$$

where the suffixes G and L refer to the gas and the liquid, respectively. The constant n_1, which can be calculated with an elliptic integral related to the eccentricity of the bubble, is equal to 1/3 for a perfect sphere, while $n_1 > 1/3$ for an oblate ellipsoid (Landau and Lifšitz, 1986). The validity of Eq. (18) stands on several restrictions: the dielectric must be isotropically, linearly and homogeneously polarizable, and both fluids must have zero conductivity; besides, the bubble must be small enough to obtain the amount of polarization by approximating the field as locally uniform (Pohl, 1958; Snyder and Chung, 2000). These drawbacks were recently removed by Karayiannis and Xu (1998) who developed a more general relationship in the form of a surface integral. It must also be considered that the presence of bubbles may substantially alter the local electric field distribution with respect to the one in the absence of bubbles, so that all these effects should be carefully evaluated. If the bubble is immersed in a liquid of higher electrical permittivity, a net force arises, driving it towards the zone of weaker electric field. This force has generally a little magnitude, however in the absence of buoyancy it might be an important tool for phase separation.

A dimensionless parameter G_{be}, scaling the effect of electric force F_{DEP} to buoyancy one F_{BU}, can be defined as

$$G_{\mathrm{be}} = \frac{F_{\mathrm{DEP}}}{F_{\mathrm{BU}}} = \frac{1}{2} \frac{(\varepsilon_{\mathrm{G}} - \varepsilon_{\mathrm{L}})\varepsilon_{\mathrm{L}} \mathrm{grad}\, E^2}{[n_1 \varepsilon_{\mathrm{G}} + (1 - n_1)\varepsilon_{\mathrm{L}}](\rho_{\mathrm{L}} - \rho_{\mathrm{G}})g} \tag{19}$$

The effects of electric field on formation and departure of air bubbles in cyclohexane was experimentally theoretically and numerically studied by Cho et al. (1996) and by Kweon et al. (1998). Uniform and non-uniform field distributions were investigated, as well as A.C. and D.C. fields. They observed that with a uniform field the increase of the applied voltage caused the bubbles to elongate in the field direction during the growing period, with almost no effect on their detachment volume. In the case of non-uniform electric field they observed a decrease in detachment volume as the voltage increased, with almost no elongation during detachment. A.C. electric fields were found more effective than D.C. ones in promoting bubble departure.

Herman et al. (2002) investigated the effect of a nearly uniform electric field on air bubbles injected into a fluoroinert liquid (PF5052, which is analogous to FC-72) through an orifice of 1.5 mm diameter, with $1.81 < We^* < 6.15$. The experimental campaign was performed in microgravity in parabolic flight, with a minimum gravity level of $3 \times 10^{-3}\ g_0$, and a relevant g-jitter. They observed that bubble elongation increased almost linearly with the applied voltage, while bubble detachment volume decreased more than predicted by their theoretical model.

2. Experimental apparatus

2.1. Experimental facility

As previously mentioned, in order to separate the mechanical effects from the thermal and mass exchange ones, adiabatic two-phase flow conditions were established by injecting gas bubbles in a liquid through an orifice. To achieve a good level of microgravity conditions, the apparatus was operated in the Japan Microgravity Center (JAMIC) dropshaft, located at Kamisunagawa in Hokkaido (JAMIC, 1995). A free drop length of 490 m ensures over 10 s of free fall with a g-level near $10^{-4}g_0$, with a very low g-jitter (see also Table 1). Two identical cells sharing the auxiliary devices were arranged in a "half size" JAMIC standard rack, in order to double the number of available tests. Each experimental cell consisted of an aluminum box of about 2.5 dm^3 volume monitored by temperature and pressure sensors, connected to a bellows in order to allow for volume dilatation due to temperature changes and gas injection, without leaving a free surface above the liquid (see Fig. 2). Each cell was provided with windows on two sides and on the upper part, to allow visualization and video shots of phenomena occurring inside. The adopted fluid was FC-72 (C_6F_{14}) a fluoroinert liquid manufactured by 3M, used in electronics cooling. In order to avoid gas dissolution in the liquid during bubble growth, the fluid was gas-saturated before the tests by means of extensive and prolonged bubbling. The geometry of the test section was derived from the one of an analogous apparatus operated at Pisa University, to study boiling phenomena (Di Marco and Grassi, 1999), in order to compare the results. It consisted mainly of a horizontal copper tube (1 mm o.d., 0.2 mm i.d.) connected to the gas injection device. The two cells were identical except for the orifice diameter d_0: in the following cell 1 refers to $d_o = 0.15$ mm while, for cell 2, $d_o = 0.13$ mm. The nitrogen was injected from a pressurized vessel into the fluid via the

Table 1
Test matrix (g-level was evaluated by JAMIC data acquisition system)

LOG	Cell	Applied voltage (kV)	Fluid temperature (°C)	Pressure (kPa)	g-level ($10^{-4}g_0$)	Volume flow rate (mm^3/s)	We^*	Detachment frequency (Hz)		Acquisition time (s)	Frame rate, fram/s	Resolution, pix/mm
								At 1 g	In μg			
1711	1	0	24.0	104.4	4.4	10.03	0.00513	38.5	n.a.	6.89	500	20.5
1722	2	0	25.9	102.1	2.4	9.21	0.00657	43.5	n.a.	8.3	1000	18.4
1822	2	0	26.7	103.0	3.6	43.25	0.147	105.3	n.a.	8.3	1000	18.4
1812	1	1	25.7	103.7	3.6	10.12	0.00518	46.2	n.a.	6.89	500	24.0
1811	1	2.5	22.9	103.6	6.5	10.07	0.00511	41.7	1.52	8.3	1000	20.4
1222	2	3.5	22.4	100.1	1.9	9.31	0.00646	47.6	2.5	8.3	1000	26.2
1712	1	5	25.5	103.8	2.4	10.23	0.00534	60	11.5	6.89	500	20.4
1122	2	7.5	24.8	100.6	1.9	9.32	0.00658	102.0	41.3	8.3	1000	26.2
1821	2	10	23.4	103.4	6.5	8.93	0.00610	111.1	91.7	8.3	1000	18.4
1221	2	12.5	21.3	100.4	2.6	9.39	0.00657	129.6	111.2	8.3	1000	26.2
1721	2	15	24.7	103.0	4.4	9.02	0.00632	130	110.2	6.89	500	18.4
1521	2	18	15.8	102.7	2.3	9.07	0.00612	157.1	119.7	3.4	1000	26.0

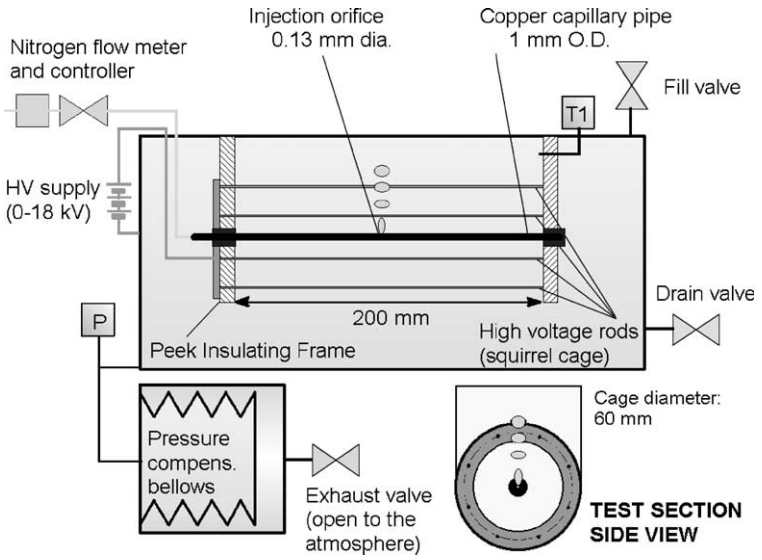

Fig. 2. Sketch of the test apparatus.

orifice drilled in the upper part of the tube. The electric field was generated by imposing a D.C. potential drop V (0–18 kV) to a eight-rod cylindrical squirrel cage surrounding the tube, which was grounded. The resulting electric field was nearly cylindrical in geometry:

$$E = k\frac{V}{r} \tag{20}$$

where V is the applied potential and r the radial distance from the tube axis. Finite elements calculations (Danti, 2000) showed that Eq. (20) is valid up to $r = 12$ mm and the constant k is 0.172.

Bubbles generated from the orifice of each cell were recorded with a NAC high-speed video camera, set to a frame rate from 500 to 1000 fps. In this way, the bubbling phenomena occurring in microgravity during 6–8 s were observed with a resolution ranging from 18 to 26 pixel/mm. In addition, pressure, temperature and gas flow rate inside each cell were measured and recorded by the data acquisition system of JAMIC. To measure and control nitrogen mass flow, a digital mass flow controller (model El-Flow by `Bronkhorst`) was used in each cell: this device guaranteed a stable inlet mass flow (proportional to an input voltage) in the chamber below the orifice. The outlet flow rate from the orifice stabilized at the same value within some seconds. The gas volume flow rate was calculated by means of the measured values of temperature and pressure. The apparatus was intended to work in "fixed flow" conditions; these were achieved mainly by reducing the volume of the gas chamber under the orifice. The conditions to ensure "fixed-flow" operation in the apparatus are discussed in detail by Danti et al. (2000). The flow in each cell was adjusted in order to have approximately the same detachment frequency in zero field conditions. Beside, a single test was carried out at very high gas flow rate in order to promote bubble detachment in microgravity. The complete test matrix is summarized in Table 1.

2.2. Data reduction and measurement uncertainties

The physical quantities deduced from the video images were the bubble detachment frequency, center of mass velocity and equivalent diameter.

Time measurements with the camera are affected by one frame resolution, which corresponds to $\delta_t = 2$ ms or 1 ms for the frame rates used, i.e. 500 or 1000 fps.

The detachment frequency, f, comes from the period, defined as the temporal distance between two completely detached bubbles; since these are not always detected at the same distance from the orifice, a statistical treatment is needed to get a consistent value and calculate the error. The number of bubbles considered to get a period measurement was so chosen to reduce the contribution of statistical fluctuations lower than the resolution limit, when possible. The error Δf was then calculated as the sum of the two contributions as

$$\Delta f = \frac{\sqrt{\delta_t^2 + \sigma_t^2}}{T_0^2} \tag{21}$$

where T_0 is the detachment period and σ_t is the sample standard deviation over the measurements.

Image processing was then performed using a free-ware software (Scion Image), working with binary images.

A threshold method was used for edge detection (after contrast enhancing). The brightness histogram showed two peaks corresponding to the background and the gray level typical of the bubbles. The threshold level was chosen as the middle of two peaks.

This method was confirmed to yield good results on spherical and elliptical objects of known volume and enabled us to measure N (number of pixels in a bubble) and p (number of pixels in its perimeter). The center-of-mass coordinates of a bubble were defined as

$$x_G = \frac{1}{N}\sum_i \sum_j x_i \Theta(x_i, y_j), \qquad y_G = \frac{1}{N}\sum_i \sum_j y_i \Theta(x_i, y_j) \tag{22}$$

where x and y are pixel coordinates (x-axis in the gravity direction) and $\Theta(x, y)$ is a function whose value is 1 if (x, y) is within a bubble and 0 otherwise.

The error on these measurements is mainly due to lines/columns counting: if the bubble is enclosed in a rectangular frame whose dimension in pixels are a (x-direction) and b (y-direction), the uncertainties in the coordinates center of mass are $\delta_{x_G} = 1/\sqrt{b}$ and $\delta_{y_G} = 1/\sqrt{a}$.

The vertical velocity was obtained from two frames (not necessarily two consecutive ones) taken at times t_1 and t_2

$$u = (x_{G2} - x_{G1})/(t_2 - t_1) \tag{23}$$

This value was assigned at the point whose vertical coordinate is $x = (x_{G2} + x_{G1})/2$, and errors were evaluated by using a propagation rule as

$$\left(\frac{\Delta u}{u}\right)^2 = \frac{\delta_{x_{G2}}^2 + \delta_{x_{G1}}^2}{(x_{G2} - x_{G1})^2} + \frac{\Delta t_1^2 + \Delta t_2^2}{(t_2 - t_1)^2} \tag{24}$$

The volume of the bubble was evaluated as

$$V = 2/3 \cdot (\text{projected area}) \cdot (\text{max axis}) = 2/3 \cdot (N - p/2 - 1) \cdot (b - 1) \tag{25}$$

considering the contour passing in the middle of each perimetral pixel and bubbles as oblate ellipsoids with b as the major axis. The calculated values showed a plateau as long as the bubble path kept rectilinear. A mean over this region was taken as the detachment volume. The error was derived (considering $p/2$ as the area error) as

$$\Delta V = \frac{p}{2(N - p/2 - 1)} V \tag{26}$$

Finally, the equivalent diameter was obtained by using Eq. (8) and its error was given by

$$\frac{\Delta d_{eq}}{d_{eq}} = \frac{1}{3} \frac{\Delta V}{V} \tag{27}$$

The unit of length in the above calculations was in pixels (velocities in pixel/s and volumes in pixel^3), so that a conversion factor was needed to change the length unit into metrical units. This was measured from a gauge image, taken before the test in the same optical conditions, featuring a steel bar with ticks at known distances and introduced a new source of errors to be propagated. This error was added at the final stage to the previous ones and was mainly statistical (due to mechanical differences in ticks, differences in the light distribution etc.).

The resulting uncertainties are reported as error bars in the data plots, when possible. Typical uncertainties in equivalent diameter and aspect ratio measurement were around 2%, and those in velocity (for a single bubble) ranged from 3% to 4.5%.

3. Results and discussion

A total of eight drops were performed in JAMIC during four days (two in the year 2000 and two in 2001), for a total of sixteen combinations of experimental parameters. The test matrix, referring to the 11 tests relevant for this study, is given in Table 1. The injection of nitrogen was started 40 s before the drop: in this way, the flow controller stabilized the flow rate to the desired value before the onset of microgravity. Video recording was started about 1 s before the drop, and a recording time of 7.25 or 8.77 s was achieved, depending on the adopted field of view and frame rate. Shortly before delivering the apparatus to JAMIC personnel, tests in normal gravity were performed in the same experimental conditions for comparison.

The results without electric field indicated that, as soon as microgravity was established, no detachment of the bubble occurred in both cells in the tests at low flow rates (tests 17-1-1, 17-2-2): the bubble grew as a perfect sphere attached to the orifice during the entire drop (see Fig. 3). Conversely (Fig. 4), by increasing the flow rate (test 18-2-2), three large bubbles detached during the entire drop, each of them followed by several satellite small bubbles. The three main bubbles were slightly different in size: the first one was the larger and had a diameter of 6.8 mm. As a regime condition was not attained during the 10-s drop, it was not possible to define a detachment frequency in this case.

The trend of the bubble volume vs. time in the three tests with no electric field applied is shown in Fig. 5. The trend of the volume vs. time of the growing bubble attached to the orifice is compared with the gas volume entering the test tube, obtained as the measured inlet volume flow rate multiplied by the elapsed time. It can be seen that the volume of the bubble is always greater

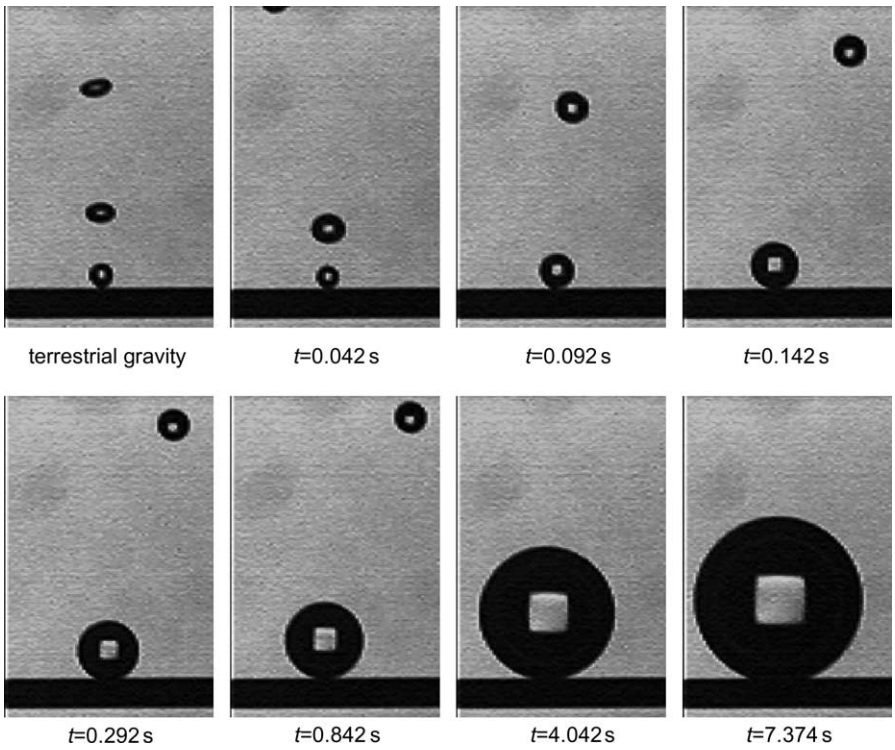

Fig. 3. Growing bubble with no detachment at low flow rate (9.2 mm^3/s) in test 17-2-2 (no electric field applied). Flow pattern in normal gravity is reported for comparison. The tube diameter (black line at the bottom) is 1 mm and t is the time elapsed from the beginning of the drop.

than the second one. This might be ascribed to the inertia of the chamber underneath the orifice or to the difference in density between the gas in the chamber and the gas in the bubble, due to the pressure drop across the orifice. Besides, the trend of the bubble volume vs. time is not linear, thus evidencing the delaying effect of the chamber and possibly the inertial effects of the surrounding liquid.

As already outlined, Pamperin and Rath (1995) on the basis of a simple force balance evidenced that the detachment of the bubble in microgravity should occur when the modified Weber number (see Eq. (14)) exceeds a critical value, $We^* > 8$. In the present case, no detachment occurred at a low flow rate ($We^* = 0.006$), but the detachment occurred at the higher flow rate of $We^* = 0.147$, i.e. far less than the theoretical value. Even Herman et al. (2002) noted the detachment of bubbles in the absence of electric field for We^* lower than the one given by Pamperin and Rath, and postulated a role of the g-jitter (which is relevant in parabolic flight) in triggering it. Since the level and quality of the residual gravity acceleration in the present experiment is similar to the one of Pamperin and Rath, both the experiments were performed with a very low g-jitter level in a dropshaft, the encountered difference might be ascribed to a smaller contact angle for the fluoroinert fluid, which is very well wetting. It is worth remarking that, according to Eq. (13), the critical Weber number decreases with decreasing contact angle, vanishing for contact angle equal

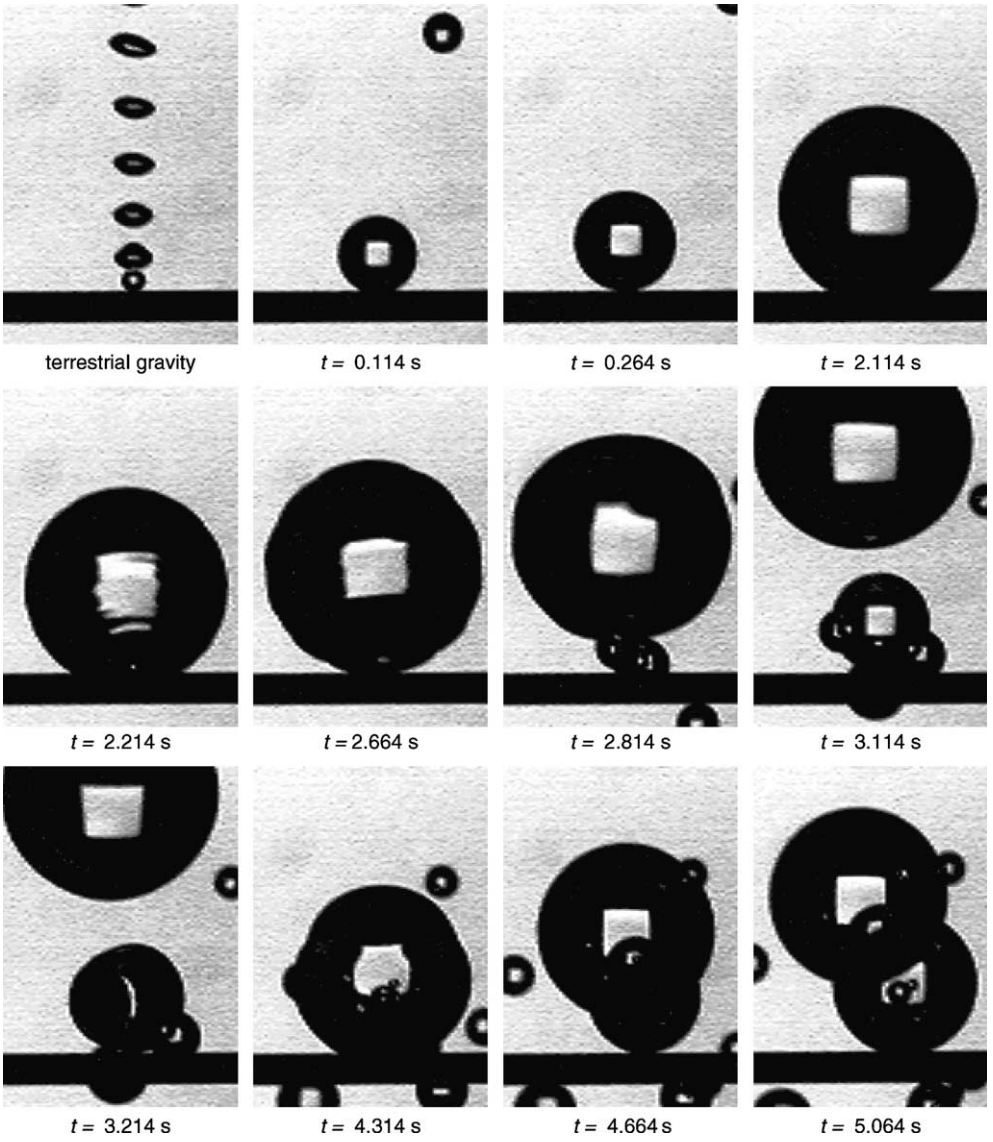

Fig. 4. Growth and detachment of bubbles at high flow rate (43.3 mm^3/s) in test 18-2-2 (no electric field applied). Flow pattern in normal gravity is reported for comparison. The tube diameter (black line at the bottom) is 1 mm and t is the time elapsed from the beginning of the drop.

to zero. The action of different forces than the ones included in the model of Pamperin and Rath (1995) can also be considered, taking into account the different geometry and the fact that these forces can come into play in this case, due to the above-mentioned reduction of contact angle. In particular, from the analysis of the high speed images, it is observed that marked interfacial waves started to develop on the bubble surface before its detachment (see Fig. 4). This surface instability may trigger an earlier bubble detachment than predicted by the simple model (Eq. (13)). Similar interfacial instabilities were also observed by Herman et al. (2002).

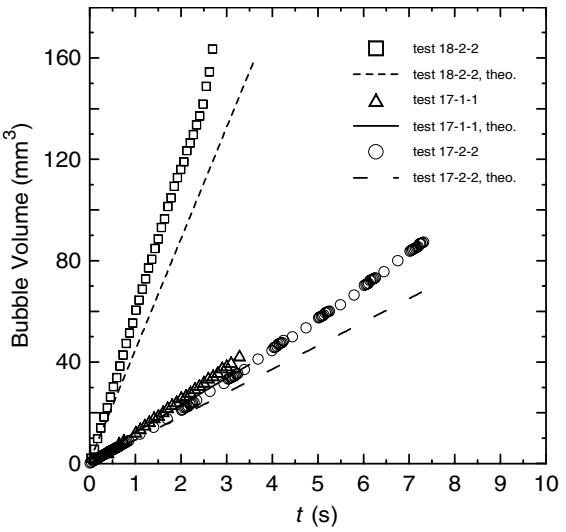

Fig. 5. Bubble volume vs. time in microgravity, no electric field applied. Experimental uncertainties are of the same order as the symbol size.

By applying the electric field, detachment of bubbles was obtained in all the microgravity tests: however, the bubble size and detachment frequencies changed with gravity acceleration, and these changes were less evident at the higher values of the applied voltage. The values of the detachment diameter in normal gravity normalized to the one at zero electric field are plotted vs. the applied voltage in Fig. 6. The data are also compared with the prediction of a model derived after

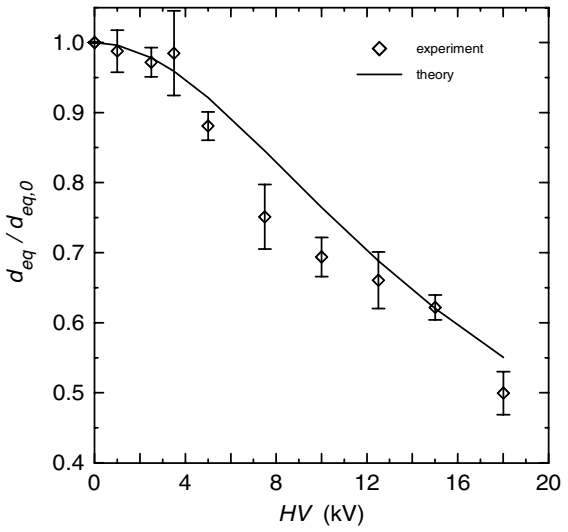

Fig. 6. Bubble detachment diameter (normalized to the one in terrestrial gravity with no field applied) vs. applied electric voltage in terrestrial gravity, and comparison with the model by Baboi et al. (1968).

Baboi et al. (1968) (Danti et al., 2000). This model accounts for balance of buoyancy, surface tension and electric force (neglecting the Coulombic one), for a spherical bubble, resulting in an expression of the detachment diameter d_{det}

$$d_{\mathrm{det}} = h(\theta)\sqrt{\frac{\sigma}{(\rho_{\mathrm{L}} - \rho_{\mathrm{G}})g}}\left[1 + \frac{3(\varepsilon_{\mathrm{G}} - \varepsilon_{\mathrm{L}})\varepsilon_{\mathrm{L}}\mathrm{grad}\,E^2}{8\pi(\varepsilon_{\mathrm{G}} + 2\varepsilon_{\mathrm{L}})(\rho_{\mathrm{L}} - \rho_{\mathrm{G}})g}\right]^{-0.5} \tag{28}$$

where $h(\theta)$ is a function of the contact angle. It is worth noting that when the second term in square bracket prevails, the detachment diameter becomes independent of gravity.

The detachment diameters in micro-gravity condition, normalized to the one in terrestrial gravity for the same value of the electric field, are plotted vs. the applied voltage in Fig. 7. Detachment of bubbles occurred for all the values of the applied field. It can be seen that for HV $>$ 10 kV, there was no difference in detachment diameter between micro and normal gravity conditions: this demonstrates the dominance of the electrical force over the buoyancy one in these conditions. For HV $<$ 10 kV, the detachment diameter increased in microgravity: presumably the threshold where detachment ceases to occur is a little below the lowest value of voltage tested (1 kV, test 18-1-2): only very few and large bubbles detached in these conditions.

The rising velocity of the bubbles is shown in Fig. 8 for normal gravity conditions and in Fig. 9 for microgravity conditions. For the higher values of the applied electric field, the velocity exhibited a peak and then decreased with distance. This is ascribed to the fact that the intensity of the electrical force, due to the field geometry, decreases with increasing radius at it was almost negligible at a distance from the tube greater than about 2–3 mm, where all the curves merged with the zero-field one. Afterwards, the geometry of the field results in a slowing-down effect on bubbles. For the same reasons, in microgravity conditions the rising velocity of the bubbles decreased to zero with increasing distance from the orifice. It should be noted that the peak velocity

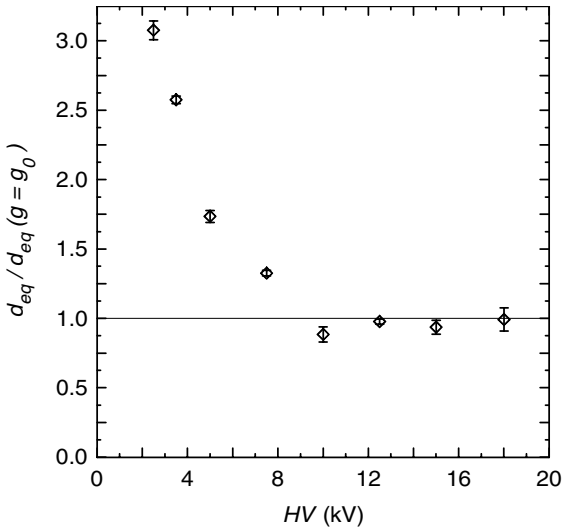

Fig. 7. Bubble detachment diameter (normalized to the value in terrestrial gravity for the same field) vs. applied electric voltage, in microgravity.

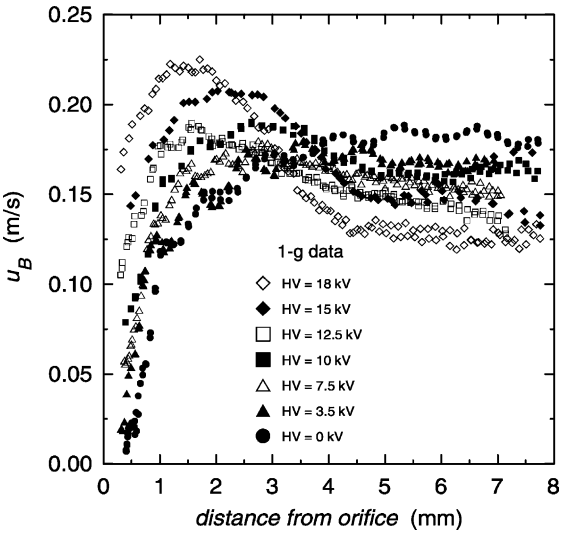

Fig. 8. Bubble rising velocity (in tests with a flow rate of about 9 mm^3/s) vs. distance from the orifice, normal gravity. Experimental uncertainties range from 3% to 4.5% and are not reported on the plot for the sake of clarity.

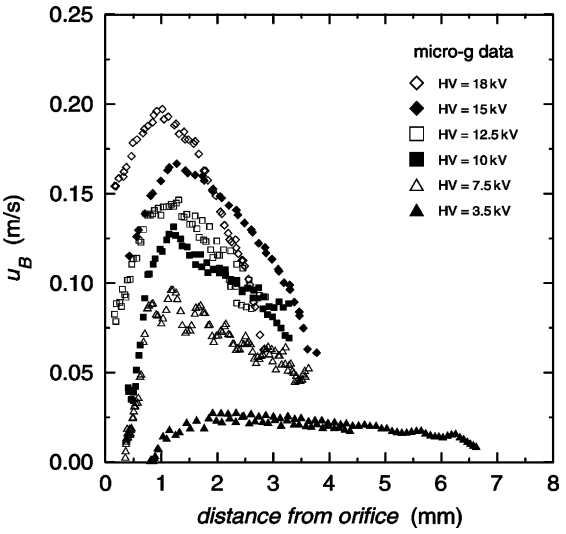

Fig. 9. Bubble rising velocity (in tests with a flow rate of about 9 mm^3/s) vs. distance from the orifice, reduced gravity. Experimental uncertainties range from 3% to 4.5% and are not reported on the plot for the sake of clarity.

at 18 kV in normal gravity (about 0.22 m/s, see Fig. 8) was still greater than the one reached in microgravity (about 0.2 m/s, see Fig. 9): this indicates a residual sensible action of the buoyancy force in the process of bubble lifting. This was not contradictory with the results concerning detachment diameter, due to the aforementioned decay of electric field with increasing distance from the orifice.

Some significant flow patterns in the presence of the electric field can be seen in Figs. 10–12. For an applied field of 5 kV, the detachment diameter is still greater in μg (Fig. 10), while at 10 and

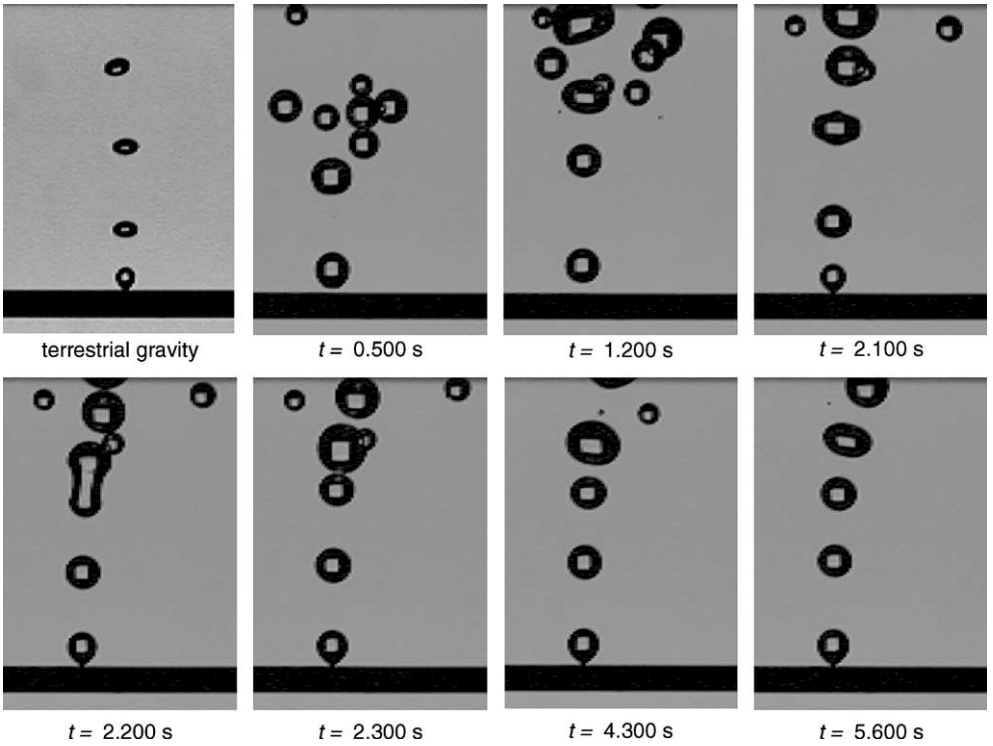

Fig. 10. Bubbling flow patterns in microgravity with 5 kV applied electric field (test 17-1-2, volume flow rate 10.22 mm^3/s). Flow pattern in normal gravity is reported for comparison. The tube diameter (black line at the bottom) is 1 mm and t is the time elapsed from the beginning of the drop.

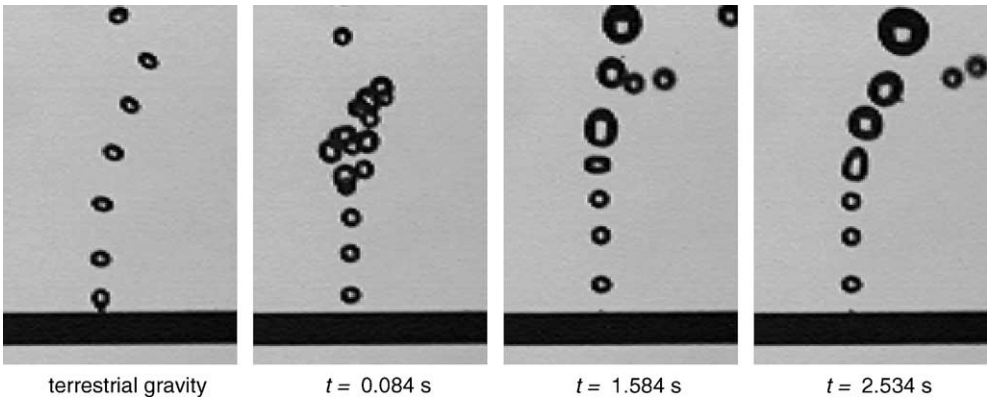

Fig. 11. Bubbling flow patterns in microgravity with 10 kV applied electric field (test 18-2-1, volume flow rate 8.93 mm^3/s). Flow pattern in normal gravity is reported for comparison. The tube diameter (black line at the bottom) is 1 mm and t is the time elapsed from the beginning of the drop.

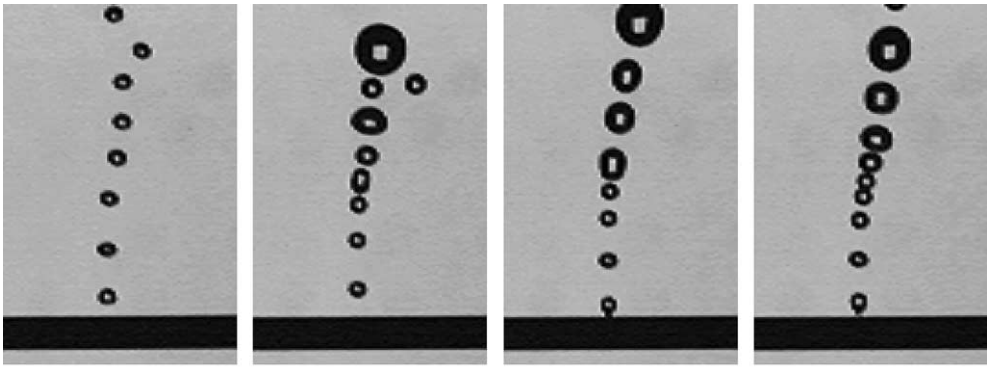

Fig. 12. Bubbling flow patterns in microgravity with 15 kV applied electric field (test 17-2-1, volume flow rate 9.02 mm^3/s). Flow pattern in normal gravity is reported for comparison. The tube diameter (black line at the bottom) is 1 mm and t is the time elapsed from the beginning of the drop.

15 kV the detachment diameter is almost independent of gravity level (Figs. 11 and 12). Bubbles tend to retain a more spherical shape in microgravity. Slowing down and coalescence of bubbles start to take place 3–4 mm away from the orifice in all these cases, as well evidenced in Fig. 10.

4. Conclusions

An experimental apparatus was set up and operated in the JAMIC dropshaft to study the influence of electrical forces on bubble dynamics in microgravity. In order to separate the mechanical effects from the thermal and mass exchange ones, adiabatic two-phase flow conditions were established by injecting nitrogen gas bubbles in a fluoroinert liquid through an orifice. The geometry of the test section and of the electric field was chosen in order to allow a future comparison with the results of a similar apparatus operated by the LOTHAR laboratory of the University of Pisa and dedicated to the investigation of boiling phenomena. Bubble size, detachment frequency and velocity were measured by digital processing of high-speed images in a total of 12 tests.

The results showed that, in microgravity and in the absence of electric field, bubble detachment did not take place at low gas flow rate; conversely at higher gas flow, the dynamical effects were sufficient to induce bubble departure. The value of detachment diameter was lower than predicted by available theoretical models and the role of surface instabilities in promoting detachment was evidenced in the images. The application of electric field showed effective in providing a force able to remove the bubbles away from the orifice and in promoting bubble departure at values of diameter greater but of the same order of magnitude as in normal gravity. For the higher values of the tested electric field, the detachment diameter was almost the same as in normal gravity.

In this way, the effectiveness of the electric forces in promoting bubble detachment and their progressive dominance over buoyancy force was experimentally demonstrated. The results obtained so far in this relatively simple experimental configuration will help in elaborating mecha-

nistic models of phase separation, bubble formation and detachment, both for adiabatic gas liquid flows and for the more complex boiling phenomena.

Acknowledgements

Thanks are due to Mr. Roberto Manetti for the design and the assembling of the electronics and for technical assistance. Authors would also like to thank the student Michele Danti who set up the apparatus and took part in the experiments in the frame of the activities of his graduation thesis. The cooperation of the direction and the personnel of JAMIC is gratefully acknowledged, as well as that of JSUP, which provided the two high-speed cameras. The work was partly funded by the Italian Space Agency (ASI) under contract ARS–99–66.

References

Allen, P.H.G., Karayiannis, T.G., 1995. Electrohydrodynamic enhancement of heat transfer and fluid flow. Heat Recovery Syst. & CHP 5, 389–423.

Baboi, N.F., Bologa, M.K., Klyukanov, A.A., 1968. Some features of Ebullition in an electric field. Appl. Electr. Phenom. (USSR) 2, 57–70.

Buyevich, Yu.A., Webbon, B.W., 1996. Bubble formation at a submerged orifice in reduced gravity. Chem. Eng. Sci. 51, 4843–4857.

Clift, R., Grace, J.R., Weber, M.E., 1978. In: Bubbles, Drops and Particles. Academic Press, p. 172.

Cho, H.J., Kang, I.S., Kweon, Y.C., Kim, M.H., 1996. Study of the behavior of a bubble attached to a wall in a uniform electric field. Int. J. Multiphase Flow 22, 909–922.

Danti, M., 2000. Master Thesis, University of Pisa.

Danti, M., Di Marco, P., Grassi, W., Memoli, G., 2000. Effect of an external electric field on bubble dynamics: Preliminary study. Proc. XVIII UIT National Conference, Cernobbio, 28–30 June, pp. 715–728.

Datta, R.L., Napier, D.H., Newitt, D.M., 1950. The properties and behavior of gas bubbles formed at a circular orifice. Trans. Instn. Chem. Engrs. 28, 14–26, as cited by Clift et al. (1978).

Davidson, J.F., Schuler, B.O., 1960a. Bubble formation at an orifice in a viscous liquid. Trans. Inst. Chem. Eng. 38, 144–154.

Davidson, J.F., Schuler, B.O., 1960b. Bubble formation at an orifice in an inviscid liquid. Trans. Inst. Chem. Eng. 38, 335–342.

Delhaye, J.M., 1980. Local instantaneous equations. In: Delhaye, J.M., Giot, M., Riethmuller, M.L. (Eds.), Thermohydraulics of Two-Phase Systems for Industrial Design and Nuclear Engineering. Hemisphere Pub. Corp., Washington (Chapter 5).

Di Marco, P., Grassi, W., 1993. Saturated pool boiling enhancement by means of an electric field. J. Enhanced Heat Transfer 1, 99–114.

Di Marco, P., Grassi, W., 1999. EHD effects on pool boiling in reduced gravity. Proc. of the 5th ASME/JSME Joint Thermal Engineering Conference, San Diego, CA, USA, paper AJTE99/6275.

Di Marco, P., Grassi, W., 2001. Pool boiling in reduced gravity. Multiphase Sci. Technol. 13, 179–206.

Di Marco, P., Grassi, W., Memoli, G., 2001. Experimental study on terminal velocity of nitrogen bubbles into FC-72. In: Celata, G.P., Di Marco, P., Goulas, A., Mariani, A. (Eds.), Experimental Heat Transfer Fluid Mechanics and Thermodynamics, 2001. pp. 1349–1359.

Di Marco, P., Grassi, W., 2002. Motivation and results of a long-term research on pool boiling heat transfer in low gravity. Int. J. Th. Sci. 7, 567–585.

Gaddis, E.S., Vogelpohl, A., 1986. Bubble formation in quiescent liquids under constant flow conditions. Chem. Eng. Sci. 41, 97–105.

Herman, C., Iacona, E., Földes, I.B., Suner, G., Milburn, C., 2002. Experimental visualization of bubble formation from an orifice in microgravity in the presence of electric fields. Exp. Fluids 32, 396–412.

Hughes, R.R., Handlosa, A.E., Evans, M.D., Maycock, R.L., 1955. Formation of bubbles at simple orifices. Chem. Eng. Prog., 577.

JAMIC, 1995. Users' Guide, Japan Microgravity Center, Kamisunagawa (J).

Karayiannis, T.G., Xu, Y., 1998. Electric field effect in boiling heat transfer. Part A: Simulation of the electric field and electric forces. Enhanced Heat Transfer 5, 217–229.

Khurana, A.K., Kumar, R., 1969. Studies in bubble formation III. Chem. Eng. Sci. 24, 1711–1723.

Kumar, R., Kuloor, N., 1970. The formation of bubbles and drops. Adv. Chem. Eng. 8, 255–368.

Kweon, Y.C., Kim, M.H., Cho, H.J., Kang, S., 1998. Study on the deformation and departure of a bubble attached to a wall in d.c./a.c. electric fields. Int. J. Multiphase Flow 24, 145–162.

Landau, L.D., Lifšitz, E.M., 1986. Electrodynamics of Continuous Media, second ed. Pergamon, New York, pp. 68–69.

Magnaudet, J., Eames, I., 2000. The motion of high-Reynolds-number bubbles in inhomogeneous flows. Ann. Rev. Fluid Mech. 32, 659–708.

Milne Thomson, L.M., 1996. Theoretical Hydrodynamics, fifth ed. Dover Publication, Mineola, NY.

Pamperin, O., Rath, H.J., 1995. Influence of buoyancy on bubble formation at submerged orifices. Chem. Eng. Sci. 50, 3009–3024.

Park, Y., Lamont Tyler, A., de Nevers, N., 1977. The chamber orifice interaction in the formation of bubbles. Chem. Eng. Sci. 32, 907–916.

Peebles, F., Garber, H., 1953. Studies on the motion of gas bubbles in liquid. Chem. Eng. Prog. 49, 88–97.

Pohl, H.A., 1958. Some effects of non-uniform fields on dielectrics. J. Appl. Phys. 29, 1182–1189.

Ramakrishnan, S., Kumar, R., Kuloor, N.R., 1969. Studies in bubble formation—I bubble formation under constant flow conditions. Chem. Eng. Sci. 24, 731–747.

Rayleigh Lord, 1920. Scientific Papers, vol. 6. Cambridge University Press. p. 504.

Satyanarayan, A., Kumar, R., Kuloor, N.R., 1969. Studies in bubble formation—II bubble formation under constant pressure conditions. Chem. Eng. Sci. 24, 749–761.

Snyder, T.J., Chung, J.N., 2000. Terrestrial and microgravity boiling heat transfer in a dielectrophoretic force field. Int. J. Heat Mass Transfer 43, 1547–1562.

Terasaka, K., Tsuge, H., 1993. Bubble formation under constant-flow conditions. Chem. Eng. Sci. 48, 3417–3422.

Tomiyama, A., 1998. Struggle with computational bubble dynamics. Proc. 3rd International Conference on Multiphase Flows (CD-ROM), Lyon, 8–12 June.

Tomiyama, A., Kataoka, I., Zun, I., Sakaguchi, T., 1998. Drag coefficients of single bubbles under normal and microgravity conditions. JSME Int. J. Series D 41, 472–479.

Tsuge, H., 1986. Hydrodinamics of Bubble Formation from Submerged Orifices, Encyclopedia of Fluid Mechanics. pp. 191–232 (Chapter 9).

Tsuge, H., Hibino, S.I., 1972. The Motion of Gas Bubbles Generating from a Single Orifice Submerged in a Liquid. Keio Engineering Reports, vol. 25, p. 7.

Tsuge, H., Terasaka, K., Koshida, W., Matsue, H., 1997. Bubble formation at submerged nozzles for small gas flow rate under low gravity. Chem. Eng. Sci. 52, 3415–3420.

Wraith, A.E., 1971. Two-stage bubble growth at a submerged orifice. Chem. Eng. Sci. 26, 1659–1671.